DOI:10.1021/jf103364a

JOURNAL OF AGRICULTURAL AND FOOD CHEMISTRY
ARTICLE

Preparation and Characterization of Durum Wheat (*Triticum durum*) Straw Cellulose Nanofibers by Electrospinning

Beatriz Montaño-Leyva,[†] Francisco Rodriguez-Felix,[‡] Patricia Torres-Chávez,*[,‡] Benjamin Ramirez-Wong,[‡] Jaime López-Cervantes,[†] and Dalia Sanchez-Machado[†]

[†]Departamento de Biotecnología y Ciencias Alimentarias, Instituto Tecnológico de Sonora, 5 de febrero entre 6 de abril y 200, Cd. Obregón, Sonora, Mexico, and [‡]Departamento de Investigación y Posgrado en Alimentos, Universidad de Sonora, Rosales y Boulevard Luis Encinas, Hermosillo, Sonora, Mexico

Cellulose nanofibers from durum wheat straw (*Triticum durum*) were produced and characterized to study their potential as reinforcement fibers in biocomposites. Cellulose was isolated from wheat straw by chemical treatment. Nanofibers were produced via an electrospinning method using trifluoroacetic acid (TFA) as the solvent. The nanofibers were 270 ± 97 nm in diameter. Analysis of the FT-IR spectra demonstrated that the chemical treatment of the wheat straw removed hemicellulose and lignin. XRD revealed that the crystallinity of the cellulose was reduced after electrospinning, but nanofibers remained highly crystalline. The glass transition temperature (T_g value) of the fibers was 130 °C, higher than that of cellulose (122 °C), and the degradation temperature of the fibers was 236 °C. Residual TFA was not present in the nanofibers as assessed by the FT-IR technique.

KEYWORDS: Durum wheat straw; cellulose; nanofiber; electrospinning

INTRODUCTION

Ecological concerns aimed at reducing the use of nonrenewable raw materials are stimulating the development of new materials from natural sources. Cellulose fibers from crops such as cotton, linen, hemp, jute, and wood have been investigated as reinforcing agents in thermoplastic matrices because of their low density, abundance, renewability, low cost, strength, and minimum abrasion of processing and transformation equipment (*1*, *2*). Agricultural residues can provide a major source of cellulose fibers. In Mexico, national wheat production is almost 4 million tons per year, of which approximately 2 million tons are durum wheat (Sistema de Información Agroalimentaria y Pesquera, http// www.siap.gob.mx). Approximately 1.6 kg of nongrain material is produced for every kilogram of grain in a wheat crop (*3*). Thus, nearly 3.2 million tons of durum wheat straw is produced in Mexico each year.

Wheat straw is primarily composed of cellulose-fiber conglomerates bound by an intercellular matrix composed of hemicelluloses, lignin, and pectins (*4*). The major component is cellulose, which chemically consists of a linear polymer formed by D-glucose units joined by β-1−4 glucosidic bonds. In nature, the cellulose chains are packed in an orderly manner to form compact microfibers, which are stabilized by both inter- and intramolecular hydrogen bonds. These microfibers have diameters of 8−10 nm and lengths of a few micrometers (*1*).

In recent years, several studies have attempted to obtain these plant nanofibers and use them to produce organoleptically desirable high-fiber foods (*5*) and biomedical materials (*6*) and to reinforce materials for biocomposites (*1*, *7*). The use of the electrospinning method to produce nanofibers has increased substantially in recent years (*6*−*12*) due to the ability to provide nanofibers directly from a polymer solution. This method is based on the ejection of a continuous stream of a polymer solution from an orifice using electrostatic forces. The liquid stream solidifies into a strand that is randomly deposited on the surface of a collector to form fibers (*11*).

Because the electrospinning method produces nanofibers directly from a polymer solution, the choice of an appropriate solvent is critical for successful nanofiber production. Cellulose exhibits very low solubility in organic solvents due to its crystallinity and its large number of hydrogen bonds, complicating the production of nanofibers by electrospinning (*12*). However, Ohkawa et al. (*6*) have successfully obtained nanofibers by electrospinning using cellulose directly solubilized with trifluoroacetic acid (TFA).

Here, we propose to utilize durum wheat straw, an abundant agricultural residue, as a raw material for the production of cellulose nanofibers. The use of these nanofibers in biomaterials may be a commercially viable application that would encourage the use of renewable sources that are currently underutilized. To this end, we produced cellulose nanofibers from durum wheat straw and characterized their dimensions and morphology using scanning electron microscopy (SEM), their chemical structure using Fourier-transform infrared spectroscopy (FT-IR), their crystallinity using X-ray diffraction (XRD), and their thermal stability using thermogravimetric analysis (TGA) and differential scanning calorimetry (DSC).

*Corresponding author [phone +52 (662) 2592207-08-09; fax +52 (662) 2592207; e-mail pitorres@guayacan.uson.mx].

 Published on Web 01/05/2011

MATERIALS AND METHODS

Extraction of Cellulose. Durum wheat straw (*Triticum durum* cv. Jupare) was processed with a mill (Thomas Wiley laboratory mill, model 4, Swedesboro, NJ) and sieved through a 180 μm mesh screen (Retsch GmbH, Haan, Germany). The straw was previously dewaxed using the Soxhlet method as described in the standards of the Technical Association of the Pulp and Paper Industry (TAPPI) (T264 om-82 and T204 os-76). Cellulose was extracted from the durum wheat straw by a method commonly used to assess the α-cellulose and hemicellulose content of lignocellulosic materials as previously described (*13*). The holocellulose content (α-cellulose + hemicelluloses) of the fibers was obtained by treating the fibers with $NaClO_3$ and NaOH (J. T. Baker, Philipsburg, NJ). The α-cellulose content of the fibers was then extracted through further NaOH treatment of the fibers to remove the hemicelluloses.

Preparation of Nanofibers. Nanofibers were prepared from the wheat straw cellulose. To prepare the nanofibers, we used TFA (Alfa Aesar, Ward Hill, MA) as a solvent, according to the method of Ohkawa et al. (*6*). To find the conditions for nanofiber formation, we tested important variables, including solvent composition, polymer concentration, flow rate, voltage, and distance between the needle and the plate collector, on the basis of the conditions reported by Okawa et al. (*6*). **Table 1** shows the conditions tested. The polymer concentration varied from 4 to 5.5% (w/v). Solvents tested were pure TFA and mixtures of TFA with water and TFA with acetic acid (Merck, Darmstadt, Germany). Mixtures were intended to diminish the volatility of the TFA. The polymer solution was then transferred to a 10 mL plastic syringe with an 0.8 mm diameter needle. Flow rate varied from 0.5 to 2.3 mL/h and was controlled by a syringe pump (K_d Scientific, Holliston, MA). A voltage between 12 and 20 kV was applied to the polymer solution using a high-voltage power supply (Spellman, CZE 1000 R, USA). Distance between the needle and the collector plate varied from 5 to 10 cm, and a square aluminum plate (10 cm ×10 cm) was used as the collector.

SEM. The morphology of the wheat straw, isolated cellulose, and nanofibers was observed using a scanning electron microscope (JEOL 5410LV, Tokyo, Japan) at an acceleration voltage of 15 kV. Materials were sputtered-coated with carbon prior to examination. The average diameter of the fibers was determined in 3 samples and 30 fibers randomly taken on each one. The program Image Tool version 3.0 was used.

XRD. XRD analyses were carried out using an X-ray diffractometer (Rigaku Geiger-flex D/Max-B, Tokyo, Japan) equipped with Cu Kα radiation and a graphite monochromator at a scanning rate of 0.02°. Wheat straw, cellulose, and nanofibers were analyzed from $2\theta = 5°$ to $2\theta = 70°$ with a step size of $2\theta = 0.02°$ at 40 kV and 20 mA.

FT-IR Spectroscopy. FT-IR spectroscopy was used to examine the structural changes in the cellulose fibers and nanofibers. A Perkin-Elmer spectrum GX spectroscope (Perkin-Elmer Life and Analytical Sciences Inc., Waltham, MA) was used to obtain the spectra of each sample. Fibers were milled, mixed with KBr (Aldrich Chemicals, Milwaukee, WI), and pressed into thin, transparent pellets. FT-IR spectroscopic outputs were collected in the range of 4000−400 cm^{-1}. Spectral outputs were recorded in transmittance mode as a function of wavenumber.

Thermal Characterization. TGA and DSC were performed to study the degradation characteristics and glass-transition temperatures (T_g) of the wheat straw, cellulose, and nanofibers. Determinations were carried out on simultaneous DSC−TGA equipment (TA Instruments, SDT 2960, New Castle, DE). A 6 mg sample of each material was heated to 700 °C at a heating rate and cooled at a cooling rate of 10 °C/min. Nitrogen was used as a purge gas at a flow rate of 20 mL/min. Three repetitions of the measurements were done.

Statistical Analysis. Descriptive statistics and analysis of variance at a significance level of 95% were performed with the statistical software XLSTAT-2010 (Addinsoft Corp.).

Table 1. Electrospinning Conditions Tested in the Preparation of Nanofibers from Wheat Straw Cellulose

sample	polymer concentration (wt %)	solvent	collector distance (cm)	flow rate (mL/h)	voltage (kV)
WSC[a]	4.0	TFA[b]/water	10.0	0.9	15
WSC	4.0	TFA/water	10.0	1.5	15
WSC	4.0	TFA/acetic acid	10.0	1.5	15
WSC	4.0	TFA[b]	10.0	0.8	15
WSC	4.0	TFA	10.0	1.5	15
WSC	4.0	TFA	10.0	2.0	17
WSC	4.0	TFA	10.0	2.5	15
WSC	4.0	TFA	5.0	1.5	15
WSC	4.0	TFA	7.0	1.5	15
WSC	5.0	TFA	5.0	1.5	15
WSC	5.0	TFA	5.0	0.5	17
WSC	5.0	TFA	7.0	1.5	15
WSC	5.5	TFA	5.0	1.5	15
WSC	5.5	TFA	7.0	1.5	15

[a] WSC, wheat straw cellulose. [b] TFA, trifluoracetic acid. Solvent mixture TFA/water 9:1; TFA/acetic acid 9:1.

RESULTS AND DISCUSSION

Electrospinning Conditions. Conditions for electrospinning were identified on the basis of the homogeneity of the fibers and their direction with respect to the collector plate. Conditions for nanofiber formation were a polymer concentration of 4.0%, pure TFA as a solvent, a needle-to-collector-plate distance of 7.0 cm, a flow rate of 1.5 mL/h, and a voltage of 15 kV. Appearance of the nanofibers was similar to that described by Ohkawa et al. (*6*): a white sheet with a fine structure similar to that of a nonwoven fabric composed of nanoscale fibers and tubular aggregates. When mixtures of TFA with water and TFA with acetic acid were used to solubilize the cellulose, drops were produced instead of fibers, probably due to the incomplete evaporation of the solvent.

SEM and Physical Characteristics. Figure 1A shows that wheat straw was formed of cellulose−fiber conglomerates that were tightly joined by an intercellular matrix composed of hemicelluloses, lignin, and pectins. Wheat straw also contained a large amount of silica, located mostly in the epidermis (*4*). To extract cellulose fibers, hemicellulose, lignin, and pectins must be removed. We isolated cellulose using the treatment described by Zobel and McElvee (*13*). SEM examination demonstrated that cellulose fibers were successfully isolated (**Figure 1B**), showing residue-free fibers. Additionally, **Figure 1C** shows that after chemical treatment, the cellulose−fiber conglomerates could be separated more easily.

The average diameter of the cellulose−fiber conglomerates was 42 ± 0.68 μm (**Figure 1B**). This result is consistent with the diameter of the same structures of wheat straw (25−125 μm) reported by Hornsby et al. (*4*). In this study, the average diameter of individual wheat straw cellulose fibers was 5 ± 1.17 μm, smaller than that of the fibers produced by Alemdar and Sain (10−15 μm) (*1*).

Nanofibers are defined as submicrometer fibers having diameters varying from 100 to 500 nm (*14*). SEM micrographs of the cellulose nanofibers (**Figure 1D−F**) showed a continuous tubular morphology with mean diameters of 270 ± 0.097 nm. The nanofibers obtained by Ohkawa et al. (*6*) from cotton and wood-pulp cellulose using TFA as a solvent had smaller diameters (30−50 nm). Nanofibers can be utilized to reinforce biomaterials because their small diameters confer an extremely high specific surface area, up to 1000 times larger than the surface area of microfibers (*15*), and permit direct contact between cellulose and matrix polymers. On the other hand, because of their small diameter, these nanofibers may achieve stability by grouping themselves into larger fibrous structures, as can be seen in this

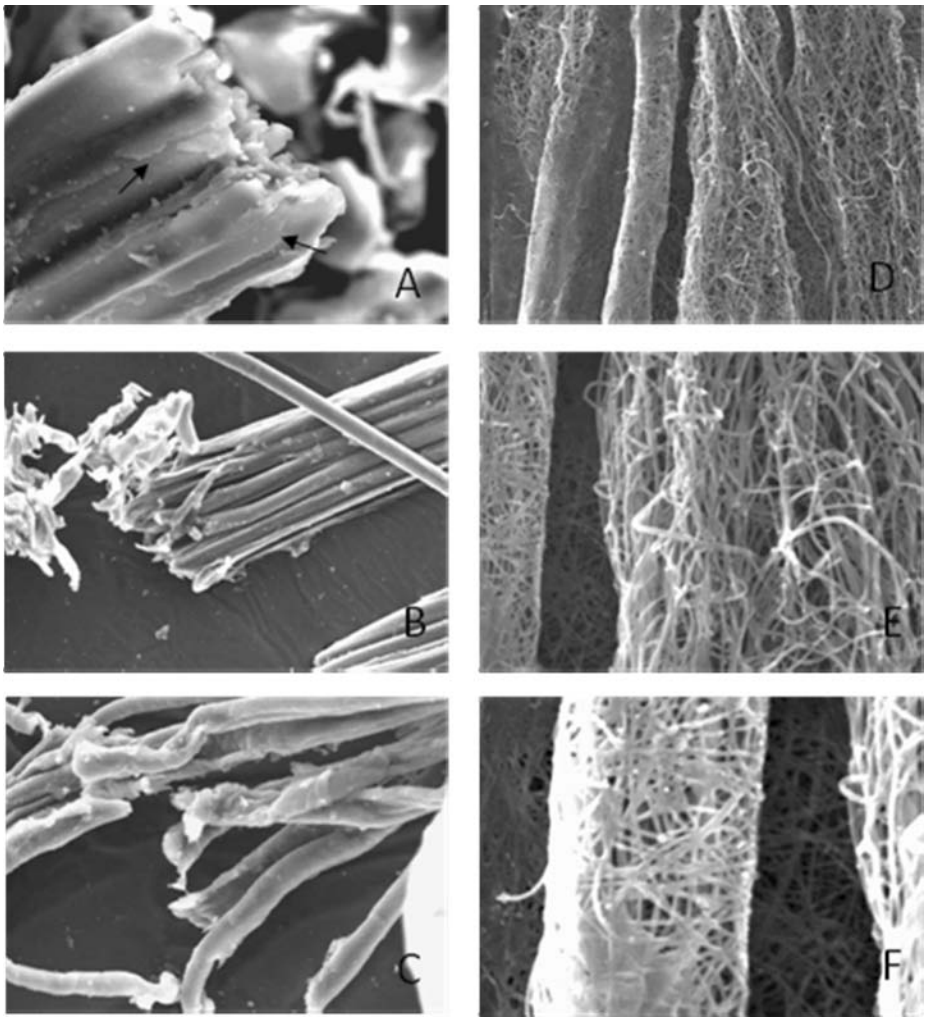

Figure 1. Scanning electron micrographs of (**A**) durum wheat straw without treatment (magnification, 2000×), (**B** and **C**) cellulose fibers obtained after chemical treatment (magnification 700× and 1500×, respectively), and (**D**, **E**, and **F**) electrospun cellulose nanofibers (1500×, 5000×, 7500×, respectively). Silica is indicated by arrows in **A**.

study. Some of the nanofibers obtained from wheat straw exhibit a structural rearrangement in tubular aggregates, as shown in **Figure 1D−F**. The lower left section of the tubular aggregate (**Figure 1F**) appears to show collapsed fibers. This can be the result of incomplete drying of the TFA. Tubular aggregates may increase the tensile strength of the fibers; however, this may reduce the surface area or may also interfere with a proper dispersion of the nanofibers in the matrix, a requisite for the reinforcing performance of the nanofibers (*16*). This needs to be investigated.

FT-IR Spectroscopy. FT-IR spectroscopy is a nondestructive method used to study the physicochemical properties of lignocellulosic materials (*1*). **Table 2** shows the main FT-IR bands presented by the materials under study. FT-IR analysis of both the cellulose and nanofibers revealed changes in their structure. In the spectrograms (**Figure 2**), a band of strong intensity at ∼3400 cm^{-1} was observed due to the stretching of the O−H bonds, and a band of medium intensity at ∼2800 cm^{-1} was attributed to the stretching of C−H bonds (*1*). In the spectrum for durum wheat straw (**Figure 2A**), a prominent band at 1734 cm^{-1} could be attributed to the uronic esters and acetyl groups from the hemicelluloses or to the ester bonds of the carboxylic groups of the ferulic and *p*-coumaric acids from lignin (*17*). This peak disappeared in the cellulose fibers (**Figure 2B**), indicating that the isolation method effectively broke the ester bonds of the hemicelluloses and lignin, thereby removing them. The band at 1509 cm^{-1} (**Figure 2B**) was attributed to vibrations of the aromatic ring of lignin (*17*), and this band also disappeared in the cellulose and nanofibers. The band observed at approximately 1430 cm^{-1} were attributed to CH_2 bending of cellulose and lignin (**Figure 2 A**); however, in **Figure 1B**,**D**, it was attributed only to cellulose, due to the disappearance of bands at 1734 and 1509 cm^{-1} attributed to hemicelluloses and lignin. The weak band at 1380 cm^{-1} was assigned to O−H bending (*18*). The absorbance in the 1330−970 cm^{-1} region was due to C−O bond stretching (*19*), whereas the band at 1320 cm^{-1} was produced by C−C and C−O skeletal vibrations (*20*). At 1050 cm^{-1}, a strong band attributed to the skeletal vibration of the C−O−C pyranose ring was observed (*21*). The band at 1630 cm^{-1} was attributed to the bending mode of the absorbed water in the samples (*18*). A band at 900 cm^{-1} is characteristic of the β-glucosidic bonds between sugar units (*22*). An increase of this peak indicated the typical structure of cellulose (**Figure 2B**) (*1*). At the same time, absorbances at 1429, 1372, 1318, 1164, 1061, 1034, and 901 cm^{-1} are associated with distinct cellulose peaks (*18*). Sugiyama et al. (*23*) have found absorption bands at 750 and 710 cm^{-1} for type I cellulose; these bands are assigned to phases I_α and I_β, respectively. We did not detect an absorption band at 750 cm^{-1} in the FT-IR spectra of the wheat straw cellulose; only a small band appeared at 712 cm^{-1}, indicating that phase I_β cellulose is the predominant form in the durum wheat straw.

Table 2. Main FT-IR Bands Presented by the Materials under Study

	intensity of the band			
vibration (cm^{-1}), functional group	durum wheat straw	cellulose	nanofibers not exposed to air	nanofibers exposed to air
~3400, O—H stretch	strong	strong	strong	strong
~2800, C—H stretch	medium	medium	medium	medium
~1790, C═O TFA[a]			medium	
~1734, −C═O of ester	weak			
~1630, H—O—H bendig	medium	medium	strong	medium
~1509, aromatic ring	weak			
~1430, $-CH_2$ bending	weak	weak	weak	weak
~1380, O—H bending	weak	weak	weak	weak
~1050, C—O—C stretch	strong	strong	strong	strong

[a] TFA, trifluoroacetic acid.

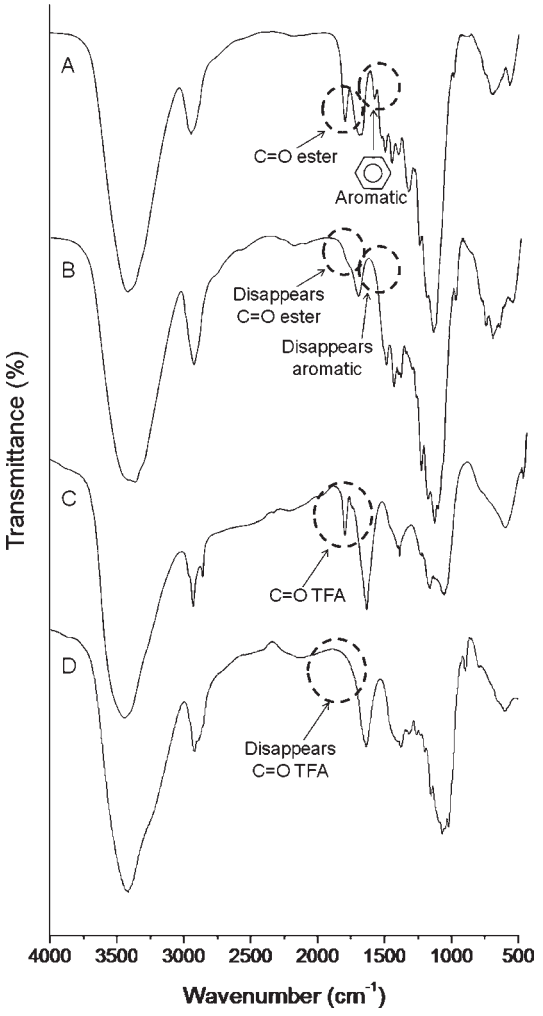

Figure 2. FT-IR spectra of the (**A**) durum wheat straw, (**B**) cellulose, (**C**) nanofibers, and (**D**) nanofibers after being exposed to air.

The FT-IR spectrum also indicated structural changes in the nanofibers obtained by electrospinning (**Figure 2C**). These changes were due to breaking of the fibrillar structure as a consequence of dissolution in TFA. Nuclear magnetic resonance spectroscopy (C NMR) revealed that when cellulose was dissolved in TFA, it formed trifluoroacetyl esters selectively at the alcohol on carbon 6 of cellulose (*24*). This observation is consistent with the results of the IR analysis of the nanofibers, in which an absorption band appeared at approximately 1790 cm^{-1} due to the carbonyls of the trifluoroacetyl ester groups. Hasegawa et al. (*24*) have demonstrated that the degree of substitution of the trifluoroacetyl groups

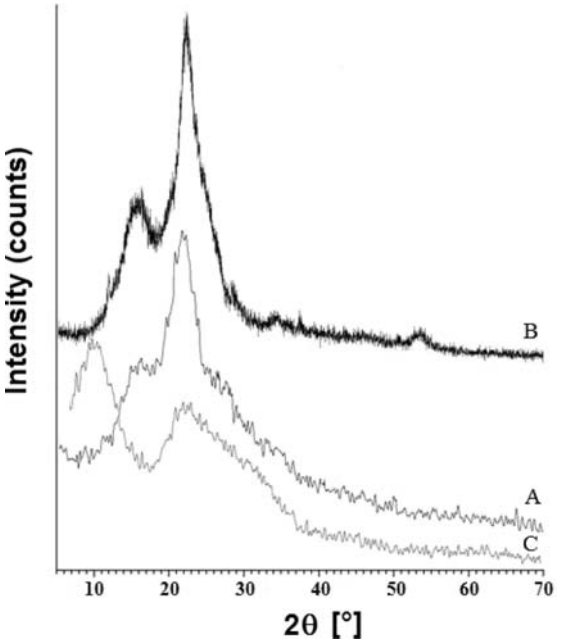

Figure 3. X-ray diffraction patterns of (**A**) durum wheat straw, (**B**) cellulose, and (**C**) nanofibers.

formed during the dissolution of cellulose decreases as the solution is exposed to air. The authors reported that the trifluoroacetyl ester groups can be gradually hydrolyzed by moisture in the air, and therefore the TFA is removed by natural evaporation. We can say that this band appeared because the nanofibers obtained in this study were analyzed without previous exposure to air. However, this band disappeared as the nanofibers were exposed to air (**Figure 2D**).

XRD. The chemical treatments and processing to which the cellulose fibers were subjected resulted in changes in X-ray diffraction patterns (**Figure 4**) ,which indicates changes in crystalline structure of durum wheat straw upon chemical conversion to cellulose. Crystalline proportions also changed; percent crystallinity calculated from the areas under the peaks and the amorphous region in the graphics were 37% for wheat straw, 62% for cellulose fibers, and 52% for cellulose nanofibers. Hydrogen bonds between cellulose molecules are arranged in a regular and ordered system, giving the cellulose crystalline properties (*1*). The crystalline system of cellulose is monoclinic; individual fibrillar units are arranged in long periods of ordered regions (crystallites) interrupted by completely disordered regions. These crystal structures in the cellulose fibers are affected by both chemical and mechanical treatments (*1*). In wheat straw, (**Figure 3A**) a crystalline organization was observed as a result of the structural

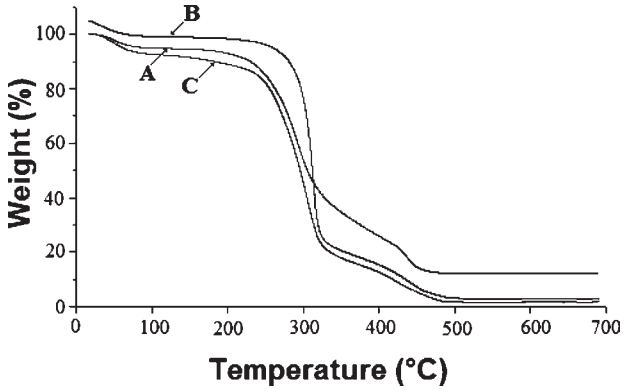

Figure 4. TGA thermograms of (**A**) durum wheat straw, (**B**) cellulose, and (**C**) nanofibers.

system of cellulose within the straw. However, the diffraction peaks were sharper in the extracted cellulose (**Figure 3B**). The sharpness of the diffraction peaks indicated a greater degree of crystallinity in the structure due to the removal of hemicelluloses and lignin during the chemical extraction (*1*).

On the other hand, diffractograms showed that the durum wheat straw cellulose (**Figure 3B**) had a type I crystal structure (characteristic peaks at $2\theta = 14.7°$, 16.4°, and 22.5°), corresponding to the native crystal structure of cellulose. This crystal form presents the greatest degree of both intra- and intermolecular hydrogen bonding (*25*). During the electrospinning process, the crystal structure of native cellulose was disorganized, apparently reducing crystallinity of the nanofibers upon deposition (**Figure 3C**). Amorphous phases in the nanofibers originated because most hydrogen bonds (intra- and intermolecular) were destroyed when the cellulose was dissolved (*26*). According to Ohkawa et al. (*6*), TFA breaks the type I crystal structure. The crystalline nature of the cellulose nanofibers can be given not only by the chain conformation but also by the packing of adjacent chains (*27*). In the nanofiber diffractogram (**Figure 3C**), two peaks were observed ($2\theta = 9.8°$ and 22.0°), probably indicating that part of the native cellulose crystal structure was retained (peak $2\theta = 22.5°$). However, the peak at $2\theta = 9.8°$ may have been the result of a structural rearrangement during the electrospinning process.

Thermal Characterization. Investigating the thermal properties of natural fibers is important in evaluating their potential use in the processing of biomaterials, when temperatures may exceed 200 °C (*1*). In this study, the glass transition temperature (T_g) and the thermal decomposition of fibers and nanofibers were measured by DSC and TGA, respectively. The T_g values obtained by DSC were significantly different ($p < 0.05$) for wheat straw (138.7 °C), cellulose (122.2 °C), and nanofibers (130.4 °C). The higher T_g value of wheat straw than those for cellulose and nanofibers can be explained by the existence of other polymers that were joined by intra- and intermolecular bonds, resulting in fewer free spaces between the polymer chains. The higher T_g value of the nanofibers than that of cellulose was probably due to the reorganization of the nanofibers in larger tubular structures (**Figure 3**). According to Rodríguez et al. (*28*), an increase in T_g can be also attributed to cross-linking of the polymer chains. We hypothesize that a structural rearrangement occurred during the production of the nanofibers, involving crystalline structure changes and leading to a large number of interactions between the polymer chains. By definition, a higher temperature would be required for the polymer chains to have greater free space and mobility.

The thermogravimetric study involved analyzing the weight loss of the material as a function of temperature. The thermograms obtained by TGA (**Figure 4**) showed that the first weight loss occurred at approximately 100 °C and amounted to a 6% degradation of the sample. This loss was attributed to the loss of moisture and solvent from the material (*29*). Thermograms of the cellulose and nanofibers presented similar behavior (**Figure 4B**,**C**). In the ranges of 246−336 °C for cellulose and 237−328 °C for nanofibers, significant weight loss occurred (∼70% of weight). Canche-Escamilla et al. (*30*) have stated that this loss is due to depolymerization of the cellulose caused by breaking of the glucosidic bonds of the chain, forming levoglucosan (1,6-anhydro-β-D-glucopyranose) and carbon residues. However, in the ranges of 337−475 °C for cellulose and 328−412 °C for nanofibers, weight decreased by ∼19%; this weight loss was attributed before to the degradation of of lignin (*30*). The thermogram of the wheat straw (**Figure 4A**) indicated greater resistance to degradation in the range of 314−446 °C due to the presence of larger amounts of hemicelluloses and lignin.

On the other hand, the degradation temperatures of the durum wheat straw, cellulose, and nanofibers were 192, 246, and 236 °C, respectively (**Figure 4**), indicating that the thermal stability of the material increased after chemical treatment during cellulose isolation. Similar behavior has been reported by Alemdar and Sain (*1*) in wheat straw that had been chemically treated. However, the degradation temperature of the nanofibers was lower than that of cellulose. The reduced crystallinity of the nanofibers may be the reason for the reduced thermal stability. Finally, the residue remaining above 700 °C amounted to 12% of the wheat straw but only about 2% of the cellulose and nanofibers. According to Nguyen et al. (*31*), the higher degradation temperature of cellulose and the smaller amount of residue are related to the partial removal of hemicelluloses and lignin in addition to the high crystallinity of cellulose. These factors explain the smaller amount of residue observed in the cellulose and nanofiber samples above 700 °C.

An application of the nanofibers as reinforcing materials in biocomposites intended for human contact or consumption is feasible. FT-IR results showed the complete removal of the TFA; thus, contact with or consumption for humans is safe. Therefore, the idea of an application in materials that can be in contact with food is reasonable. A reinforcing capability of the nanofibers can be expected from their exceptional thermal stability, high proportion of crystalline structure, and the high surface area generated with the formation of the nanofibers. This extensive area of contact with the compatible matrix ensured the strengthening of the material.

Cellulose fibers were successfully isolated by a method commonly used to assess the α-cellulose content of lignocellulosic materials. However, the use of reagents such as sodium chlorite must be properly handled (due to the high irritability produced), as well as the management of its waste into the environment. Nanofibers were obtained from durum wheat straw cellulose using the electrospinning method. Structural changes were observed in the cellulose due to the breaking of its fibrillar structure during its dissolution in TFA and posterior rearrangement. The thermal stability, high crystallinity, and extremely high contact surface generated because of their small size make the nanofibers produced from wheat straw appropriate to reinforce biomaterials as one of the possible applications. Residual TFA was not present in the nanofibers as assessed by the FT-IR technique.

ACKNOWLEDGMENT

We are grateful to Monica Castillo Ortega for providing the electrospinning equipment and to Francisco Brown Bojórquez for providing the facilities for XRD and SEM analyses.

LITERATURE CITED

(1) Alemdar, A.; Sain, M. Biocomposites from wheat straw nanofibers: morphology, thermal and mechanical properties. *Compos. Sci. Technol.* **2008**, *68*, 557−565.

(2) Rocha, G. J. M.; Balczó, N. K.; Vacaro, C.; Rodrigues, R. C. L. B. Obtainment and characterization of cellulose from sugarcane bagasse pretreated in acid medium for the synthesys of hidroxypropylmethyl cellulose (HPMC). Congreso Iberoamericano de Investigacion en Celulosa y Papel (CIADICYP), Posadas, Argentina, 2002.

(3) Martínez-Dodda, J. I. Distribución de residuos de trigo. Infocampo. Semanario agropecuario de circulación nacional. Ed.ial Perfil − California 2715 (C1289ABI). Ciudad Autónoma de Buenos Aires, Argentina, 2008; Vol. 217, p 11.

(4) Hornsby, P. R.; Hinrichsen, E.; Tarverdi, K. Preparation and properties of polypropylene composites reinforced with wheat and flax straw fibers. Part I. Fiber characterization. *J. Mater. Sci.* **1997**, *32*, 443−449.

(5) Fung, W. Y.; Yuen, K. H.; Liong, M.-T. Characterization of fibrous residues from agrowastes and the production of nanofibers. *J. Agric. Food Chem.* **2010**, *58*, 8077−8084.

(6) Ohkawa, K.; Hayashi, S.; Nishida, A.; Yamamoto, H. Preparation of pure cellulose nanofiber via electrospinning. *Text. Res. J.* **2009**, *79*, 1396−1401.

(7) Gindla, W.; Keckesb, J. All-cellulose nanocomposite. *Polymer* **2005**, *46*, 10221−10225.

(8) Kim, J. S.; Reneker, D. H. Mechanical properties of composites using ultrafine electrospun fibers. *Polym. Compos.* **1999**, *20*, 124−131.

(9) Son, W. K.; Youk, J. H.; Park, W. H. Preparation of ultrafine oxidized cellulose mats via electrospinning. *Biomacromolecules* **2004**, *5*, 197−201.

(10) Sill, T. J.; Von-Recum, H. A. Electrospinning: applications in drug delivery and tissue engineering. *Biomaterials* **2008**, *29*, 1989−2006.

(11) Tungprapa, S.; Jangchud, I.; Supaphol, P. Release characteristics of four model drugs from drug-loaded electrospun cellulose acetate fiber mats. *Polymer* **2007**, *48*, 5030−5041.

(12) Kriegel, C.; Arrechi, A.; Kit, K.; McClements, D. J.; Weiss, J. Fabrication, functionalization, and application of electrospun biopolymer nanofibers. *Crit. Rev. Food Sci. Nutr.* **2008**, *48*, 775−797.

(13) Zobel, B.; McElvee, R. Variation of cellulose in loblolly pine. *Tappi J.* **1966**, *49*, 383−387.

(14) Patel, D. B.; Rahul, D.; Prashant, K. P.; Sandip, T.; Rajeshwar, V. K. Nanofibers as drug delivery system. *Pharm. Res.* **2009**, *2*, 1184−1187.

(15) Huang, Z. M.; Zhang, Y. Z.; Kotaki, M.; Ramakrishna, S. A review on polymer nanofibers by electrospinning and their applications in nanocomposites. *Compos. Sci. Technol.* **2003**, *63*, 2223−2225.

(16) Wang, B.; Sain, M. Isolation of nanofibers from soybean source and their reinforcing capability on synthetic polymers. *Compos. Sci. Technol.* **2007**, *67*, 2521−2527.

(17) Sun, X. F.; Xu, F.; Sun, R. C.; Fowler, P.; Baird, M. S. Characteristics of degraded cellulose obtained from steam-exploded wheat straw. *Carbohydr. Res.* **2005**, *340*, 97−106.

(18) Sun, X. F.; Sun, R. C.; Su, Y.; Sun, J. X. Comparative study of crude and purified cellulose from wheat straw. *J. Agric. Food Chem.* **2004**, *52*, 839−847.

(19) Xiao, B.; Sun, X. F.; Sun, R. C. Chemical, structural, and thermal characterization of alkali-soluble lignins and hemicelluloses, and cellulose from maize stems, rye straw, and rice straw. *Polym. Degrad. Stab.* **2001**, *74*, 307−319.

(20) Pastorova, I.; Boon, J. J.; Arisz, P. W.; Boon, J. J. Cellulose char structure − a combined analytical PY-GC MS, FTIR, and NMR study. *Carbohydr. Res.* **1994**, *262*, 27−47.

(21) Pappas, C.; Tarantilis, P. A.; Daliani, I.; Mavromustakos, T.; Polissiou, M. Comparison of classical and ultrasound-assisted isolation procedures of cellulose kenaf from *Hibiscus cannabinus* L. and eucalyptus (*Eucalyptus rodustrus* Sm.). *Ultrason. Sonochem.* **2002**, *9*, 19−23.

(22) Gupta, S.; Madan, R. N.; Bansal, M. C. Chemical composition of pinus caribaea hemicellulose. *Tappi J.* **1987**, *70*, 113−114.

(23) Sugiyama, J.; Persson, J.; Chanzy, H. Combined infrared and electron diffraction study of the polymorphism of native cellulose. *Macromolecules* **1991**, *24*, 2461−2466.

(24) Hasegawa, M.; Isogai, A.; Onabe, F.; Usuda, M. Dissolving states of cellulose and chitosan in trifluoroacetic acid. *J. Appl. Polym. Sci.* **1992**, *45*, 1857−1863.

(25) Kim, C. W.; Frey, M. W.; Marquez, M.; Joo, Y. L. Preparation of submicron-scale, electrospun cellulose fibers via direct dissolution. *J. Polym. Sci., Polym. Phys.* **2005**, *43*, 1673−1683.

(26) Zhang, H.; Wu, J.; Zhang, J.; He, J. 1-Allyl-3-methylimidazolium chloride room temperature ionic liquid: a new and powerful nonderivatizing solvent for cellulose. *Macromolecules* **2005**, *38*, 8272−8277.

(27) Bhatnagar, A.; Sain, M. Processing of cellulose nanofiber-reinforced composites. *J. Reinf. Plast. Compos.* **2005**, *24*, 1259−1268.

(28) Rodríguez, F.; Castillo-Ortega, M. M.; Encinas, J. C.; Grijalva, H.; Brown, F.; Sánchez-Corrales, V. M.; Castaño, V. M. Preparation, characterization, and adsorption properties of cellulose acetate−polyaniline membranes. *J. Appl. Polym. Sci.* **2009**, *111*, 1216−1224.

(29) Castillo-Ortega, M. M.; Romero-García, J.; Rodríguez, F.; Nájera-Luna, A.; Herrera-Franco, P. J. Fibrous membranes of cellulose acetate and poly(vinylpyrrolidone) by electrospinning method: preparation and characterization. *J. Appl. Polym. Sci.* **2010**, *116*, 1873−1878.

(30) Canché-Escamilla, G.; De los Santos-Hernández, J. M.; Andrade-Canto, S.; Gómez-Cruz, R. Obtención de celulosa a partir de los desechos agrícolas del banano. *Inf. Tecnol.* **2005**, *16*, 83−88.

(31) Nguyen, T.; Zavarin, E.; Barrall, E. M. Thermal-analysis of lignocellulosic materials. 1. Unmodified materials. *J. Macromol. Sci. Rev. Macromol. Chem. Phys.* **1981**, *20*, 1−65.

Received for review August 31, 2010. Revised manuscript received December 9, 2010. Accepted December 13, 2010.